Phase Diagram Of Solid-Phase Transformation In Amorphous Carbon Nanorods.

ARTICLE *in* THE JOURNAL OF PHYSICAL CHEMISTRY A · JUNE 2014

Impact Factor: 2.69 · DOI: 10.1021/jp502928g · Source: PubMed

2 AUTHORS:

Anastassia Sorkin

Nanyang Technological University

25 PUBLICATIONS **235** CITATIONS

SEE PROFILE

Haibin Su

Nanyang Technological University

174 PUBLICATIONS **2,109** CITATIONS

SEE PROFILE

THE JOURNAL OF PHYSICAL CHEMISTRY A

Article

pubs.acs.org/JPCA

Phase Diagram of Solid-Phase Transformation in Amorphous Carbon Nanorods

Anastassia Sorkin[†] and Haibin Su*[,†,‡]

[†]School of Materials Science, Nanyang Technological University, 50 Nanyang Avenue, Singapore 639798

[‡]Institute of Advanced Studies, Nanyang Technological University, 60 Nanyang View, Singapore 639673

ABSTRACT: The transformations of amorphous carbon nanorods with different diameters and densities upon heating up to different temperatures are studied with density-functional-based tight-binding molecular dynamics. Phase diagrams with assorted transformed sp^2 nanostructures depending on both temperatures and line density, under different heating treatments, are presented to place the observations in perspective. Under instant heating, the lowest line density at which a carbon nanotube can form is 8 $Å^{-1}$, while a double-walled carbon nanotube can form at a linear density of 19−20 $Å^{-1}$ and higher. Under gradual heating, both partially unzipped carbon nanotubes and carbon nanoscrolls are formed as notable intermediate structural motifs. This work sheds light on the microscopic mechanism of various sp^2 nanostructural formations with the featured motifs highlighted as important intermediates, which will serve as an important guide in producing graphene nanoribbons, single-walled and double-walled carbon nanotubes, and carbon nanoscrolls from amorphous carbon nanorods.

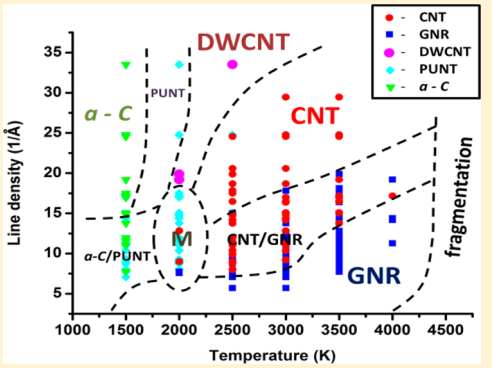

1. INTRODUCTION

Allotropes of carbon, including carbon nanotubes (CNTs)[1] and graphene,[2] together with their hybrid structures, such as peapods[3] and nanobuds,[4] are the subject of intensive investigation, due to their exceptional electronic and mechanical properties which hold promising potential for high technological impact.[5−7] Modern technologies of sp^2 carbon synthesis are mainly based on a gas-phase assembly of carbon species. The techniques for CNT growth include arc discharge,[1,6,8,9] laser ablation,[5] chemical vapor deposition (CVD),[10,11] and detonation-assisted cracking of hydrocarbons.[12] Catalytic CVD is currently the most common technique to grow both CNTs[13−18] and graphene.[19,20] The active carbon species, supplied from hydrocarbon or a-C feedstock, diffuse on the catalyst surface and form a nucleus, leading to the continuous growth of these intriguing carbon nanostructures.

Interestingly, CNTs can be also produced by the solid-phase transformation of sp^2 bonded carbon precursors. For example, double-walled CNTs could be generated in peapods by fusion of encapsulated fullerenes.[21−25] Single-walled CNTs with large diameter and multiwalled CNTs can be produced by the coalescence of single-walled CNTs with small diameter.[26−31] Very recently, the controlled fabrication schemes of producing graphene nanoribbons (GNRs) have been reported by unzipping CNTs through solution-based oxidation.[32] Furthermore, one rational approach is reported to fabricate sub-10 nm GNRs in the oxygen plasma etch process using chemically synthesized nanowires with controllable sizes down to 1 nm with a nearly atomically smooth line edge as an etch mask.[33]

With the development of modern thin film deposition and growth techniques, such as CVD, sputter deposition, and cathodic arc deposition, remarkable advancements have been made to fabricate amorphous carbon (a-C) materials.[34] Recent studies shed light on the non-catalytic graphitization of a-C nanowires and glass-carbon nanoparticles into small (∼10 nm) polycrystalline graphene,[35] and into additional shells on multiwalled CNTs.[36−38] Moreover, catalyst-free crystallization of a-C nanowires led to the formation of tubular graphitic shells with nano-onions in their interior.[39−43] Huang et al.[39] observed the conversion of amorphous carbon wires into multiwall carbon nanotubes in real time by using a scanning tunneling microscope. They applied resistive Joule heating to amorphous carbon nanowires, and found that the solid-phase transformation occurs at very high temperatures (above 2000 °C). Harris reviewed the growth of CNT in the gas phase and solid state transformations, and suggested that the heating rate is also an important parameter to promote this process.[41] Du et al.[42] also obtained multiwalled CNTs through solid-phase transformation of metal-containing glass-like carbon nanoparticles at 800−1000 °C. These experimental results also show that disordered nanoscale carbon species can be transformed into ordered sp^2 structures under very high temperatures. Zhou and Chow[43] produced carbon nanotubes by the conventional

Special Issue: International Conference on Theoretical and High Performance Computational Chemistry Symposium

Received: March 24, 2014
Revised: June 6, 2014

dx.doi.org/10.1021/jp502928g | J. Phys. Chem. A XXXX, XXX, XXX−XXX

Table 1. Transformed Carbon Nanostructures by Instantly Heating a-C Nanorods of Different Densities and Diameters to Various Temperatures

			instant heating				
density (g/cm^3)	diameter (Å)	line density (Å^{-1})	1500 K	2000 K	2500 K	3000 K	3500 K
1.7	10.87	7.67	GNR	GNR	GNR	GNR	fragmented
	11.86	8.93	damaged GNR	GNR	GNR	GNR	fragmented
	11.92	11.51	PUNT	PUNT	PUNT	GNR	GNR
	14.72	14.74	damaged GNR	PUNT	CNT	GNR	GNR
	18.24	24.77	amorphous	PUNT	PUNT	CNT	CNT
2.2	9.83	7.74	PUNT	GNR	GNR	GNR	GNR
	9.88	9.25	damaged GNR	PUNT	PUNT	GNR	GNR
	11.73	11.58	amorphous	PUNT	PUNT	GNR	GNR
	13.82	15.07	amorphous	PUNT	PUNT	CNT	CNT
	17.16	24.55	amorphous	PUNT	CNT	CNT	CNT
2.8	7.40	7.06	PUNT	fullerene with hole	GNR	GNR	fragmented
	9.49	8.75	PUNT	loop	GNR	GNR	GNR
	9.95	11.95	amorphous	PUNT	CNT	GNR	GNR
	12.72	14.85	amorphous	PUNT	open tube	CNT	GNR
	13.75	17.50	amorphous	PUNT	CNT	loop	GNR
3.2	7.85	8.01	PUNT	PUNT	CNT	GNR	GNR
	7.93	8.94	PUNT	PUNT	CNT	GNR	GNR
	8.37	10.37	PUNT	PUNT	CNT	CNT	GNR
	9.96	13.76	amorphous	PUNT	CNT	GNR	CNT
	10.93	17.16	amorphous	PUNT	loop	open tube	CNT
3.5	6.57	7.77	amorphous	damaged GNR	GNR	GNR	GNR
	6.76	9.29	PUNT	PUNT	damaged GNR	GNR	GNR
	6.83	11.04	amorphous	PUNT	CNT	CNT	GNR
	8.56	14.39	PUNT	PUNT	CNT	CNT	GNR
	8.60	16.98	amorphous	PUNT	loop	CNT	CNT
	10.12	19.19	damaged CNS	double-walled CNT	CNT	CNS	CNT
	13.03	33.51	damaged CNS	damaged CNS	double-walled CNT	CNT	CNT

carbon arc-discharge method. They proposed a two-step mechanism of carbon nanotube growth. First, the amorphous carbon assemblies with any kind of morphology such as plate, sphere, polyhedron, droplet, and cylinder with random orientation are formed in the high-temperature region on the cathode surface. Second, the graphitization occurs from the surface toward the interior of the assemblies. Shakerzadeh et al.[44] recently showed that both CNTs and graphitic nanostructures can be synthesized during physical vapor deposition. Nanostructures with preferred orientation can be produced by using a high plasma density or high substrate bias (which increase the temperature inside the thermal spike). Meanwhile, the formation of tubular structures requires both high plasma density and high substrate bias.

Disordered and crystalline carbon nanoparticles and nanowires can be transformed into sp^2 nanostructures at high temperature as unraveled by atomistic simulations,[45−54] which support the two-step solid-phase crystallization growth model.[43] In this model, amorphous carbon nanoparticles exposed to the high temperature start to graphitize from their surface, and then, the process propagates toward the interior of the particles, eventually transforming them into concentric shells of sp^2 bonded atoms forming fullerenes or multiwalled nanotubes. Powles et al.[49] performed simulations with environment-dependent interaction potential[55] to transform a-C nanostructures with various dimensionality from zero to three, controlled by geometry and density, into sp^2 bonded nanostructures. In particular, they showed that for one-dimensional amorphous precursors (i.e., nanowires) the final structure was a CNT. The simulations of a-C nanorods performed by Suarez-Martunez and Marks demonstrated that the transformation of amorphous carbon nanorods into multiwalled CNTs occurred at all densities, regardless of the nanorod shape.[53] They also found that the circumference in cross-section determines the tube diameter, with the number of walls being primarily controlled by the density of the rod. Sorkin and Su[54] performed density functional tight-binding molecular dynamics simulations[56] to transform diamond nanowires with different diameters, shapes, and orientations into CNTs and GNRs under high temperature conditions. The minimal line density of the nanotube required for formation of single-walled CNT is 7 Å^{-1}, while the formation of double-walled CNTs requires at least 25 Å^{-1}. The calculations reveal a three-stage transformation process with the intermediate structural motif of a carbon nanoscroll (CNS).[57−62] Note that CNS can also be produced in a dc arc at high temperature[57] as well as by low temperature chemical methods.[58,60,62]

Despite extensive work in this subject, the boundaries of various structures with sp^2 character are still missing, needless to mention the complete mechanism and dynamics in the whole course of transformation. Thus, it is highly desirable to carry out systematic studies on the transformation of a-C nanorods with various diameters and densities to assorted sp^2 structures, such as GNRs, CNTs, CNS, etc. The simulations are conducted with both gradual heating and instant heating up to different temperatures, by density-functional tight-binding molecular dynamics. In particular, a phase diagram, generic transformation pathways, and novel carbon nanostructures are

dx.doi.org/10.1021/jp502928g | J. Phys. Chem. A XXXX, XXX, XXX−XXX

presented, which is expected to stimulate further studies in this important field.

2. COMPUTATIONAL METHOD

The method used in this study to describe interactions between carbon atoms is the density-functional-based non-orthogonal tight-binding model[56] (DFTB) implemented in the PLATO package.[63] This method has been used for simulating the formation of various sp^2 nanostructures such as fullerenes, CNTs, and GNRs.[48,52,54] The molecular dynamics simulations are performed in the NVT ensemble. Periodic boundary conditions are applied in the direction parallel to the principle axis of a-C nanorods. The Γ-point sampling in the Brillouin zone is used for the electronic calculation. The molecular dynamics time step is 1 fs. Five samples of amorphous carbon with various densities are generated by quenching the hot gaseous carbon phase[64] with volume densities of 1.7, 2.2, 2.8, 3.2, and 3.5 g/cm^3, which correspond to 6, 15, 45, 57, and 86% of sp^3 bonded atoms, respectively, as commonly observed in amorphous carbon samples with relative densities.[65] The a-C nanorods with circle and square shaped cross-sections with different diameters are produced from these carbon networks. Then, these a-C nanorods are heated instantly to various temperatures ranging from 1000 to 4000 K for 50−100 ps. In another set of simulations, the a-C nanorods are gradually heated up to 4500 K with a heating rate of 20 K/ps. The structures are visualized with the VMD package.[66]

3. RESULTS AND DISCUSSION

The present studies show that the transformation processes depend on temperature, volume density, and diameter of a-C nanorods, and are not influenced by the shape, either circle or square, of the a-C nanorod's cross-section. Since both volume density and diameter affect transformation processes, we propose to use one new parameter, the line density, which combines the volume density and diameter as follows

$$\rho_l = \rho_v \pi r^2 / m_c \quad (1)$$

where m_c is the mass of the carbon atom and r and ρ_v are the radius and volume density of the a-C nanorods, respectively. At 1500 K, structural transformation starts to occur, while at 4000 K and above, all structures are fragmented. Therefore, the focus of this work is to establish phase diagrams of the transforming a-C nanorods into various nanostructures with respect to line density and temperature ranging from 1500 to 3500 K under both instant and gradual heating in the following sections.

3.1. Transformation of a-C Nanorods under Instant Heating. The transformed structures from a-C nanorods under instant heating at various temperatures are tabulated in Table 1. At 1500 K, a-C nanorods with high ρ_l remain to be amorphous yet with the increased ratio of sp^2 coordinated carbon atoms, while those with low ρ_l transform into partially unzipped tubular structures (PUNTs)[32,67−70] or damaged GNRs with pentagons and heptagons, and occasionally carbon chains connected to the edges. The structure of PUNT has one part like CNTs and the other as curled GNRs. Experimentally, PUNTs can be produced by treatment of CNTs and MWCNTs with sulfuric acid and potassium permanganate,[32] intercalation with lithium and ammonia,[68] and an argon plasma etching process.[69] At 2000 K, the major products are PUNTs, except a few cases ended with CNTs and GNRs, etc. (mostly for a-C nanorods with low ρ_l). At 2500 K, the percentage of CNT reaches the highest; thus, 2500 K is the desirable temperature of CNT formation in the heat induced solid transformation with a-C nanorods. With the further increase in temperature, the percentage of GNR increases for ρ_l between 7 and 23 Å^{-1}. For instance, the numbers of transformed GNRs and CNTs are almost equal at 3000 K for ρ_l being between 7 and 17 Å^{-1}. There are only a few CNTs corresponding to the initial a-C nanorods with high ρ_l; the majority are GNRs at 3500 K. Here we emphasize the importance of the introduction of ρ_l. Generally, given the volume density of a-C nanorods, there is another parameter, namely, the diameter of the nanorods, which affects the transformation. The larger diameter likely results in the higher probability of the CNT formation. For instance, two a-C nanorods with a volume density of 3.5 g/cm^3 and a larger diameter transform into double-walled CNTs (DWCNTs) between 2000 and 2500 K. The proposed ρ_l unravels the remarkable correlation with assorted transformed structures in the phase diagram presented in Figure 1.

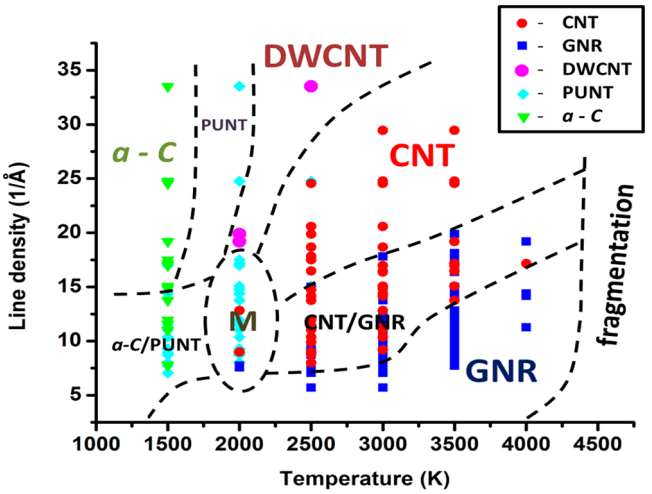

Figure 1. Phase diagram of transformation of a-C nanorods under instant heating in the line density−temperature plane. Dots with different color and shape represent various transformed products. Increasing line density promotes CNT formation. The region of several coexisting structures is labeled with M.

The phase boundaries among various sp^2 nanostructures are illustrated in Figure 1. The region of GNR formation is located at the lower right part of the diagram. Similar to the recent observation in transforming diamond nanowires to various nanostructures,[54] there exists a temperature dependent minimal ρ_l of a-C nanorods to transform into CNT, which turns out to be close to 8 Å^{-1} at 2000 K. Note that the strain energy is inversely proportional to the square of the CNT's radius. For a CNT with fixed length, its radius is proportional to the total number of carbon atoms. Therefore, the large strain energy due to the big curvature will hinder the formation of CNTs from a-C nanorods with ρ_l less than this critical value. For other a-C nanorods, the formation of CNTs is possible and subject to the heating process. At 3500 K, the minimal ρ_l for producing CNT is about 13 Å^{-1}. For a-C nanorods with ρ_l between 13 and 19 Å^{-1} at 3500 K, the final structures can be either CNT or GNR depending on the delicate integrated effects of volume density and diameter of the initial structures. Thus, there exists the two-structure, i.e., GNR and CNT, coexistence region. At a given temperature, the higher ρ_l facilitates the formation of CNT. For example, the final structure will be CNT when transforming a-

dx.doi.org/10.1021/jp502928g | J. Phys. Chem. A XXXX, XXX, XXX−XXX

C nanorods with ρ_l higher than 18 Å^{-1} at 3000 K. Moreover, for a-C nanorods with ρ_l higher than 19 Å^{-1}, the DWCNTs can be produced between 2000 and 2500 K.

The three-stage transformation mechanism of a-C nanorods under instant heating is presented in Figure 2. Similar observations have been reported in the transformation of nanodiamonds[52] and diamond nanorods.[54] The increase of kinetic energy with increasing temperature drives the structural transformation starting from the graphitization on the surface of a-C nanorods. The sp^3 carbon atoms on the surface rearrange very fast into sp^2 carbons which start to form sp^2 patches in the vicinity of exterior boundary. The newly formed sp^2 patches rapidly consolidate to form curled GNRs or PUNTs. This first stage exhibits potential energy reduction with a very high rate. The mass transfer from interior atoms to the outer sp^2 shell is characterized by the "direct-adsorption" and "push-out" mechanisms.[48] Subsequently, the system experiences structural adjustment by aligning patches mainly with sp^2 and sp carbons toward the locations readily to connect to the existing sp^2 envelope. Further transformation depends on temperature and ρ_l of a-C nanorods. In the third stage, the energy decreases relatively fast as the increase of spatial extension and the improved quality of the sp^2 envelope similar to the late stage in the solid-phase crystallization growth model.[43] PUNTs with low ρ_l do not contain enough atoms to make a closed geometry, for example, CNT; instead, they unroll into GNRs. For PUNTs with high ρ_l, the hole of PUNTs can be healed which leads to the formation of CNTs between 2500 and 3000 K. When the temperature reaches 3500 K and above, the large kinetic energy, especially of atoms near edges, makes the formation of CNT more difficult. Naturally, GNRs are mostly favored at 3500K and above. Hence, the third stage of the transformation is either PUNT-to-GNR or PUNT-to-CNT depending on ρ_l and temperature. For instance, for the a-C nanorod with a ρ_l value of 14.85 Å^{-1} (volume density of 2.8 g/cm^3 and diameter of 12.72 Å), the kinetic transformation pathway is a-C nanorod-to-PUNT-to-CNT under instant heating to 3000 K, as presented in Figure 3. For the same a-C nanorod under instant heating to 3500 K, the system exhibits an a-C nanorod-to-PUNT-to-GNR kinetic pathway, as demonstrated in Figure 4.

When forming DWCNTs, the mass transfer from the interior to the surface is remarkably rapid. To retain enough interior carbon atoms to form the interior CNTs, a larger size and volume density of a-C nanorods are desirable. In this part of the study with the total number of atoms up to 452, the lower bound of ρ_l to form DWCNT is 19 Å^{-1} with a volume density of 3.5 g/cm^3. For a-C nanorods with ρ_l less than this value, the outer sp^2 envelope will develop further by integrating interior atoms to a large extent. Since the number of remaining interior atoms is not large enough to form the inner sp^2 shell, these atoms will transfer to the surface, resulting in a CNT by the "push-out" mechanism described by Lee et al.[48] The kinetic transformation pathway of instant heating an a-C nanorod with a ρ_l value of 19.19 Å^{-1} (volume density of 3.5 g/cm^3 and diameter of 10.12 Å) to 2000 K shows three-stage character,

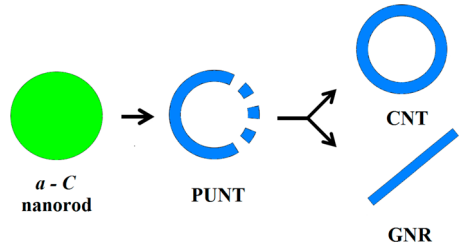

Figure 2. Pathway of transformation of a-C nanorods into ordered nanostructures. The first step of the transformation, a-C nanorod-to-opened tube or PUNT, is common for all a-C wires. Depending on the line density and heating temperature, i.e., the location of the phase diagram in Figure 1, the transformation at final stage can be either PUNT-to-CNT or PUNT-to-GNR.

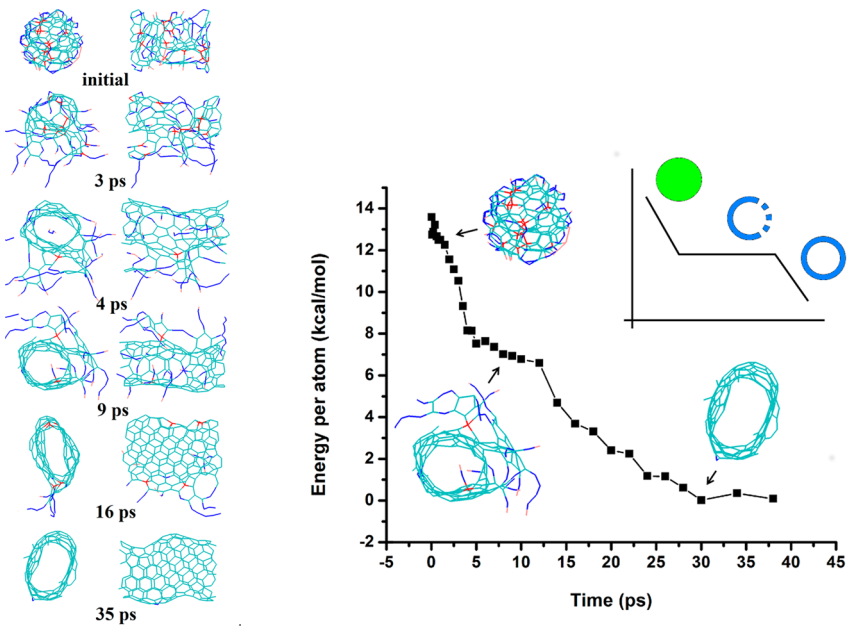

Figure 3. Transformation of the a-C nanorod with a ρ_l value of 14.85 Å^{-1} (volume density of 2.8 g/cm^3 and diameter of 12.72 Å) under instant heating at 3000 K. (a) A series of representative structures and (b) the potential energy evolution in the course of structural transformation. Clearly, three-stage transformations are revealed: a-C nanorod-to-PUNT-to-CNT, as shown in the inset.

dx.doi.org/10.1021/jp502928g | J. Phys. Chem. A XXXX, XXX, XXX−XXX

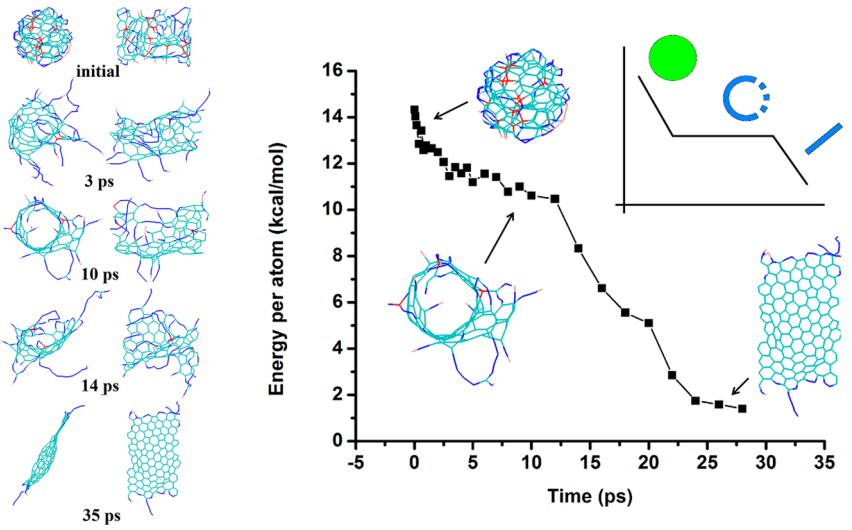

Figure 4. Transformation of the a-C nanorod with a ρ_l value of 14.85 Å^{-1} (volume density of 2.8 g/cm^3 and diameter of 12.72 Å) under instant heating at 3500 K. (a) A series of representative structures and (b) the potential energy evolution in the course of structural transformation. Clearly, three-stage transformations are revealed: a-C nanorod-to-PUNT-to-GNR, as shown in the inset.

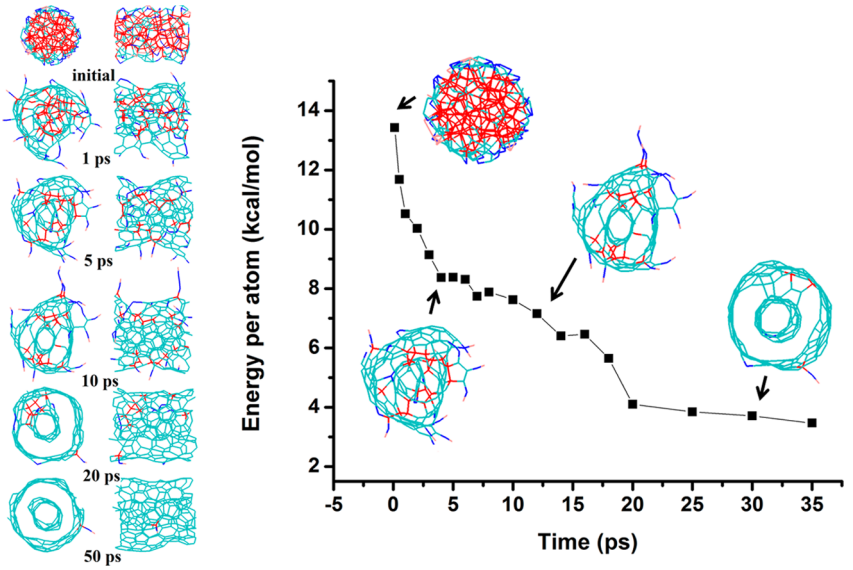

Figure 5. Formation of DWCNT by instantly heating the a-C nanorod with a ρ_l value of 19.19 Å^{-1} (volume density of 3.5 g/cm^3 and diameter of 10.12 Å) to 2000 K. (a) A series of representative structures and (b) the potential energy evolution in the course of structural transformation.

i.e., a-C nanorod-to-PUNTs-to-DWCNT, as presented in Figure 5. First, the outer sp^2 envelope, PUNT, is formed by graphitization on the surface accompanied by substantial mass transfer, quickly followed with the emergence of the inner PUNT. Subsequently, the two PUNTs experience a relatively slow gradual adjustment stage to prepare for the closing of holes in sp^2 shells. Finally, the holes of two PUNTs disappear and the concentric DWCNTs emerge. The similar inward graphitization scenario has been reported in the previous studies.[39,43,50,53,54] The threshold of ρ_l for making DWCNTs depends on the final temperature as well. As shown in Figure 1, at the higher temperature, due to the faster graphitization from the surface toward the interior, the larger ρ_l is needed to provide the required amount of interior carbon atoms for producing internal CNTs. When the total number of carbon atoms increases further, the a-C nanorods with a volume density less than 3.5 g/cm^3 and ρ_l larger than 19 Å^{-1} can be further converted into multiwalled CNTs with heat treatment, as reported by Suarez-Martinez and Marks.[53]

3.2. Transformation of a-C Nanorods under Gradual Heating. The results of a-C nanorods' transformation studied with gradual heating (20 K/ps) up to 4000 K are presented in Table 2. The intermediate structures at different temperatures in the course of the heating process are tabulated for each a-C nanorod with its specific volume density and diameter. The phase diagram illustrated in Figure 6 under gradual heating exhibits general features as those in Figure 1 under instant heating. The main differences are on DWCNT and CNS. Under gradual heating, no DWCNTs have been observed in all a-C nanorods with ρ_l up to 20 Å^{-1} and temperature ranging from 1500 to 4500 K, which is likely due to the greater flexibility and better continuous expandability of the outer sp^2 envelope with direct attachment of interior carbon atoms facilitated by gradual heating as compared with instant heating. Instead, an interesting motif, CNS, emerges for a-C nanorods

dx.doi.org/10.1021/jp502928g | J. Phys. Chem. A XXXX, XXX, XXX−XXX

Table 2. Transformed Carbon Nanostructures by Heating a-C Nanorods of Different Densities and Diameters with a Heating Rate of 20 K/ps

			gradual heating				
density (g/cm^3)	diameter (Å)	line density (Å^{-1})	1500 K	2000 K	2500 K	3000 K	3500 K
1.7	10.87	7.67	GNR	GNR	GNR	GNR	GNR
	11.86	8.93	damaged GNR	damaged GNR	GNR	GNR	GNR
	11.92	10.51	damaged GNR	PUNT	PUNT	PUNT	fullerene
	12.76	10.96	damaged GNR	damaged GNR	damaged GNR	GNR	GNR
	14.72	14.74	PUNT	PUNT	CNT	CNT	CNT
2.2	9.83	7.74	damaged GNR	damaged GNR	damaged GNR	damaged GNR	GNR
	9.88	9.25	damaged GNR	damaged GNR	damaged GNR	damaged GNR	GNR
	11.73	11.58	damaged GNR	PUNT	CNT	CNT	CNT
	13.82	15.07	amorphous	amorphous	amorphous	PUNT	CNT
2.8	7.40	7.06	damaged GNR	damaged GNR	damaged GNR	damaged GNR	GNR
	9.49	8.75	PUNT	PUNT	CNT	CNT	CNT
	9.95	11.95	PUNT	PUNT	CNT	CNT	CNT
	12.72	14.85	amorphous	PUNT	PUNT	PUNT	CNT
	13.75	17.50	amorphous	amorphous	PUNT	nano-bookshelf	nano-bookshelf
3.2	7.85	8.01	amorphous	PUNT	PUNT	PUNT	CNT
	8.37	10.37	amorphous	CNS	CNT	CNT	CNT
	9.96	13.76	amorphous	PUNT	PUNT	CNT	CNT
	10.93	17.16	amorphous	amorphous	PUNT	PUNT	CNT
3.5	6.57	7.77	damaged GNR	damaged GNR	GNR	GNR	GNR
	6.83	11.04	amorphous	CNS	CNS	CNT	CNT
	8.56	14.39	amorphous	amorphous	CNS	CNS	CNT
	8.60	16.98	amorphous	CNS	CNS	CNS	CNT
	10.12	19.19	amorphous	CNS	CNS	CNS	CNT
	10.48	19.88	amorphous	damaged CNS	CNT + GNR	loop	GNR

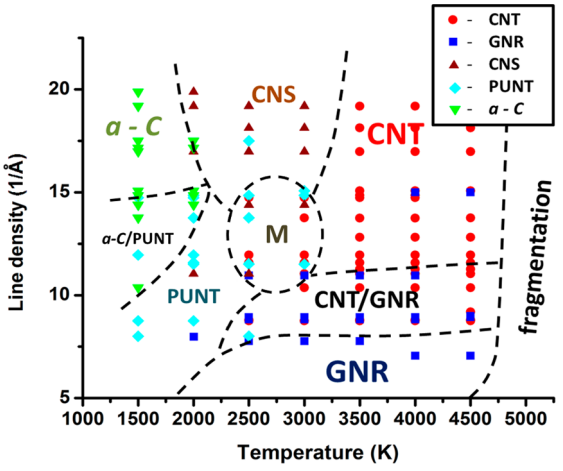

Figure 6. Phase diagram of transformation of a-C nanorods under gradual heating with a heating rate of 20 K/ps in the line density−temperature plane. Dots with different color shape represent various transformed products. Increasing line density promotes CNT formation. The region of several coexisting structures is labeled with M.

with ρ_l higher than 15 atoms Å^{-1} between 2000 and 3000 K, which is also an intermediate structure leading to CNT.[53,54] Note that data collected in gradual heating are the series of structures in the whole course of transformation with heating up to 4500 K. The phase formation temperature is relatively higher in Figure 6 as compared with that in Figure 1. For example, the formation of CNTs start from 2500 K, which usually needs 20−25 ps for a-C nanorods of less than 300 atoms with ρ_l larger than 8.8 Å^{-1}. Note that the temperature continues to rise during gradual heating. When the CNT formation is completed, the temperature already reaches 3000 K or above. Thus, the temperature of CNT formation from a-C nanorods is between 3000 and 3500 K, higher than 2500 K needed under instant heating.

For the mechanism of transformation under gradual heating, the evolution in the potential energy reveals the general three-stage character as well. The first stage starts from the graphitization of outer layers. When the temperature ranges from 1500 to 2500 K, a-C nanorods with ρ_l lower than 15 Å^{-1} transform into PUNTs. Interestingly, the CNS[57−62] appears in the samples with ρ_l higher than 15 Å^{-1} (volume density mostly of 3.5 g/cm^3) between 2000 and 3000 K. Then, sp^2 patches of PUNTs and CNSs rearrange themselves with slow reduction in the potential energy, which is the key feature of the second stage. Finally, in the third stage, PUNTs or CNSs will either unroll into GNRs or evolve into CNTs: GNRs for ρ_l less than 8 Å^{-1} and CNTs for ρ_l higher than 15 Å^{-1}. For ρ_l values between 8 and 15 Å^{-1}, the final structure being GNR or CNT depends on the delicate structural evolution details, which is influenced by the interplay among volume density and diameter of an individual a-C nanorod. For instance, for an a-C nanorod with a ρ_l value of 10.96 Å^{-1} (volume density of 1.7 g/cm^3 and diameter of 12.76 Å), the kinetic transformation pathway is a-C nanorod-to-PUNT-to-GNR, as shown in Figure 7. For a-C nanorod with a ρ_l value of 16.98 Å^{-1} (volume density of 3.5 g/cm^3 and diagonal length of 8.6 Å), the structural evolution reveals the three evident stages: a-C nanorod-to-CNS-to-CNT, as presented in Figure 8. Similar observations have been reported in the diamond nanorod transformation pathway under heat treatment, i.e., diamond nanorod-to-CNS-to-CNT.[54]

Besides the aforementioned generic mechanism, there exist two remarkable cases to illustrate the complexity due to the

dx.doi.org/10.1021/jp502928g | J. Phys. Chem. A XXXX, XXX, XXX−XXX

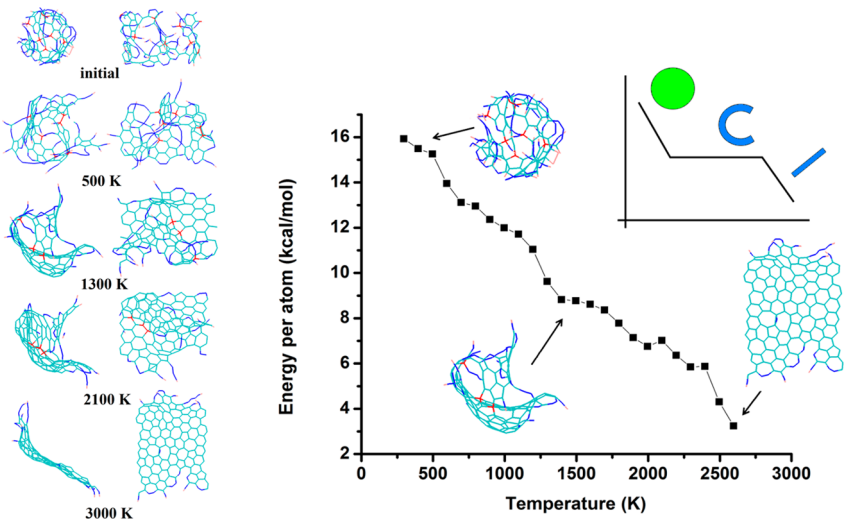

Figure 7. Transformation of the a-C nanorod with a ρ_l value of 10.96 Å^{-1} (volume density of 1.7 g/cm^3 and diameter of 12.76 Å) under gradual heating with a heating rate of 20 K/ps. (a) A series of representative structures and (b) the potential energy evolution in the course of structural transformation. Clearly, three-stage transformations are revealed: a-C nanorod-to-PUNTs-to-GNR, as shown in the inset.

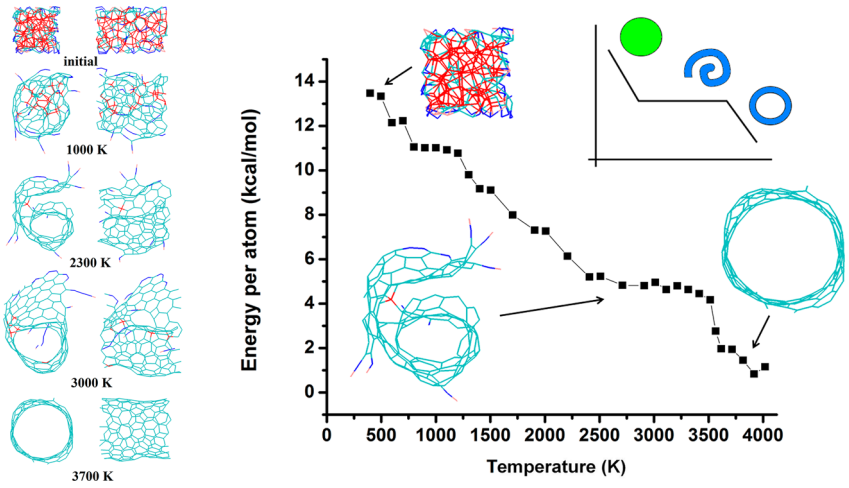

Figure 8. Transformation of the a-C nanorod with a ρ_l value of 16.98 Å^{-1} (volume density of 3.5 g/cm^3 and diagonal length of 8.6 Å) under gradual heating with a heating rate of 20 K/ps. (a) A series of representative structures and (b) the potential energy evolution in the course of structural transformation. Clearly, three-stage transformations are revealed: a-C nanorod-to-CNS-to-GNR, as shown in the inset.

emergence of junctions in the course of structural transformation. The first example is an a-C nanorod structure with a ρ_l value of 19.88 Å^{-1} (volume density of 3.5 g/cm^3 and diameter of 10.48 Å). The sp^2 shell on the surface is more dynamic and flexible under gradual heating. A CNS with a shelf-like component inside is formed, as shown in the structure at 2500 K in Figure 9. As the temperature rises, the inner part of the CNS together with the shelf form a CNT and the outer part of the CNS detaches the CNT in a form of GNR. Interestingly, the very reactive edges of the GNR anchor on the CNT through the thermal collision. This leads to the unzipping of CNT for integrating the GNR to form a longer GNR. According to the phase diagram in Figure 6, the final product should be a CNT. However, due to the formation of the junction, the system transforms into GNR instead. The second case is the a-C nanorod with a ρ_l value of 17.50 Å^{-1} (volume density of 2.8 g/cm^3 and diameter of 13.75 Å), as presented in Figure 10. Under gradual heating, the mass transfer toward the outer sp^2 shell is more significant through the "push-out" mechanism.[48] Consequently, the substantial interior carbon atoms merge into the surface to form a relatively integrated outer shell even at 2000 K as compared to the PUNT on the surface under instant heating at 2000 K. The remaining interior carbon atoms form a "nano-bookshelf" between opposite walls of the outer shell. The same nano-bookshelf structure has been produced in transforming diamond nanorods with $\langle\bar{2}11\rangle$ oriented cross-section, largely due to the graphitization of (111) facets at low temperature below 600 K.[54] The nano-bookshelf found in this work is very stable. The sp^3 bonds between the shelf and outer shell remain intact until 3800 K. Then the joints of these sp^3 bonds become broken at 4200 K. Clearly, the formation of junctions can result in special pathways, especially in the kinetic and dynamic perspectives.

4. SUMMARY

Recently, Zhang et al.[71] succeeded in growing diamond nanowires from diamantine dicarboxyl acid under extraordinary conditions inside CNTs, which provides a remarkable confinement effect, as in the carbon peapod nanostructure.[22] Inspired by this important development in preparing carbon nanowires

dx.doi.org/10.1021/jp502928g | J. Phys. Chem. A XXXX, XXX, XXX−XXX

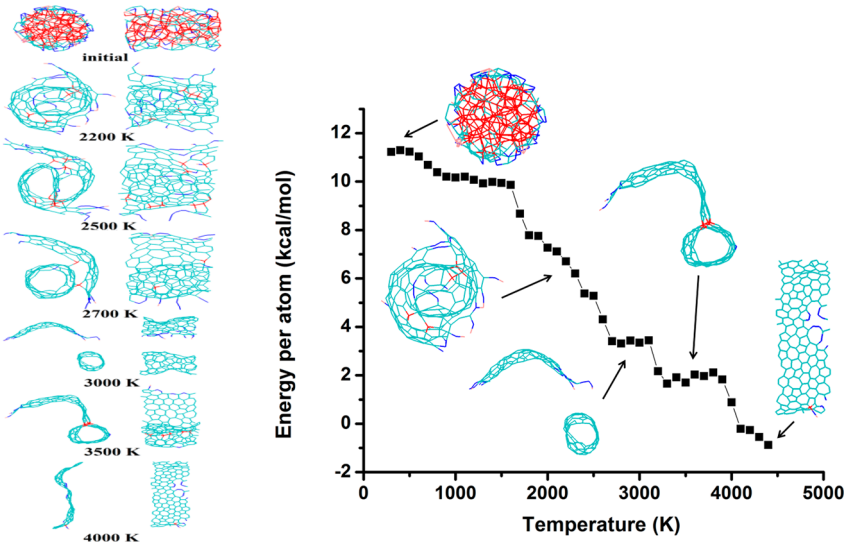

Figure 9. Transformation of the a-C nanorod with a ρ_l value of 19.88 Å^{-1} (volume density of 3.5 g/cm^3 and diameter of 10.48 Å) under gradual heating with a heating rate of 20 K/ps. (a) A series of representative structures and (b) the potential energy evolution in the course of structural transformation.

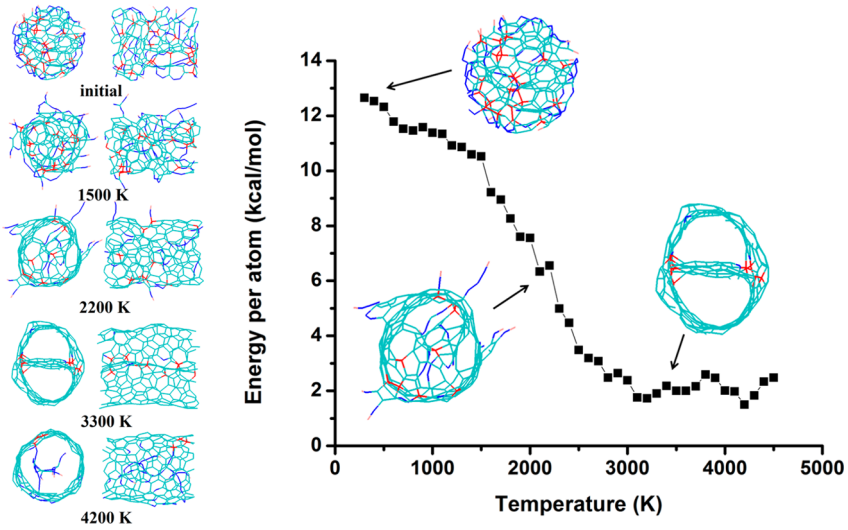

Figure 10. Transformation of the a-C nanorod with a ρ_l value of 17.50 Å^{-1} (volume density of 2.8 g/cm^3 and diameter of 13.75 Å) under gradual heating with a heating rate of 20 K/ps. (a) A series of representative structures and (b) the potential energy evolution in the course of structural transformation.

with a small number of atoms, we perform systematic studies on the transformation of a-C nanorods with various densities and diameters under instant and gradual heating. The phase diagrams are presented to place the observations in perspective. The transformation of a-C nanorods exhibits the generic three-stage-transformation characteristics. The microscopic insight of the structural transformation mechanism will hopefully guide the further endeavor in refining the phase diagrams reported in the present work.

AUTHOR INFORMATION

Corresponding Author

*E-mail: hbsu@ntu.edu.sg. Phone: +65 6790 4346. Fax: +65 6790 9081.

Notes

The authors declare no competing financial interest.

ACKNOWLEDGMENTS

We are grateful to Professor Duc Nguyen for providing the updated PLATO codes; Yang Xia and Shao-Jun Shao for helping structure analysis; and Keiji Morokuma, Hisanori Shinohara, Gehan Amaratunga, P. M. Ajayan, Manish Chhowalla, Raghu Murali, and Maziar Shakerzadeh for fruitful discussions. H.S. thanks Zeying Hu, Chinatsu Maeda, and Yilin Su for the remarkable support. Work at NTU was supported in part by SUD-Chemie AG-NTU Joint R&D award and A*STAR SERC (Grant No. 1121202012).

REFERENCES

(1) Iijima, S. Helical microtubules of graphitic carbon. *Nature* **1991**, *354*, 56−58. Iijima, S.; Ichihashi, T. Single-shell Carbon Nanotubes Of 1-nm Diameter. *Nature* **1993**, *363*, 603−605.

(2) Novoselov, K. S.; Geim, A. K.; Morozov, S. V.; Jiang, D.; Zhang, Y.; Dubonos, S. V.; Grigorieva, I. V.; Firsov, A. A. Electric Field Effect In Atomically Thin Carbon Films. *Science* **2004**, *306*, 666−669.

(3) Smith, B. W.; Monthioux, M.; Luzzi, D. E. Encapsulated C_{60} In Carbon Nanotubes. *Nature* **1998**, *396*, 323−324.
(4) Nasibulin, A. G.; Pikhitsa, P. V.; Jiang, H.; Brown, D. P.; Krasheninnikov, A. V.; Anisimov, A. S.; Queipo, P.; Moisala, A.; Gonzalez, D.; Lientschnig, G.; et al. A Novel Hybrid Carbon Material. *Nat. Nanotechnol.* **2007**, *3*, 156−161.
(5) Thess, A.; Lee, R.; Nikolaev, P.; Dai, H.; Petit, P.; Robert, J.; Xu, C.; Lee, Y. H.; Kim, S. G.; Rinzler, A. G.; et al. Crystalline Ropes of Metallic Carbon Nanotubes. *Science* **1996**, *273*, 483−487.
(6) Journet, C.; Maser, W. K.; Bernier, P.; Loiseau, A.; Lamy de la Chapelle, M.; Lefrant, S.; Deniard, P.; Lee, R.; Fischer, J. E. Large-scale Production Of Single-walled Carbon Nanotubes By The Electric-arc Technique. *Nature* **1997**, *388*, 756−758.
(7) Su, H.; Goddard, W. A., III; Zhao, Y. Dynamic Friction Force In A Carbon Peapod Oscillator. *Nanotechnology* **2006**, *17*, 5691−5695.
(8) Liu, R.−M.; Ting, J.−M.; Huang, J.−C. A.; Liu, C.-P. Growth of Carbon Nanotubes And Nanowires Using Selected Catalysts. *Thin Solid Films* **2002**, *420*−*421*, 145−150.
(9) Grobert, N. Carbon Nanotubes − Becoming Clean. *Mater. Today* **2007**, *10* (1−2), 28−35.
(10) José-Yacamán, M.; Miki-Yoshida, M.; Rendón, L.; Santiesteban, J. G. Catalytic Growth Of Carbon Microtubules With Fullerene Structures. *Appl. Phys. Lett.* **1993**, *62*, 202−204.
(11) Tans, S. J.; Devoret, M. H.; Dai, H.; Thess, A.; Smalley, R. E.; Geerligs, L. J.; Dekker, C. Individual Single-wall Carbon Nanotubes As Quantum Wires. *Nature* **1997**, *386*, 474−477.
(12) Lu, Y.; Zhu, Z. P.; Liu, Z. Y. Catalytic Growth Of Carbon Nanotubes Through CHNO Explosive Detonation. *Carbon* **2004**, *42*, 361−370.
(13) Moisala, A.; Nasibulin, A. G.; Kauppinen, E. I. The Role Of Metal Nanoparticles In The Catalytic Production Of Single-walled Carbon Nanotubes—A Review. *J. Phys.: Condens. Matter* **2003**, *15*, S3011−S3035.
(14) Bajwa, N.; Li, X.; Ajayan, P. M.; Vajtai, R. Mechanisms for Catalytic CVD Growth Of Multiwalled Carbon Nanotubes. *J. Nanosci. Nanotechnol.* **2008**, *8*, 6054−6064.
(15) Irle, S.; Ohta, Y.; Okamoto, Y.; Page, A. J.; Wang, Y.; Morokuma, K. Milestones in Molecular Dynamics Simulations Of Single-Walled Carbon Nanotube Formation: A Brief Critical Review. *Nano Res.* **2009**, *2*, 755−767.
(16) MacKenzie, K. J.; Dunens, O. M.; Harris, A. T. An Updated Review of Synthe Parameters And Growth Mechanisms For Carbon Nanotubes In Fluidized Beds. *Ind. Eng. Chem. Res.* **2010**, *49*, 5323−5338.
(17) Tessonier, J.-P.; Su, D. S. Recent Progress on the Growth Mechanism of Carbon Nanotubes: A Review. *ChemSusChem* **2011**, *4*, 824−247.
(18) Yuan, Q.; Xu, Z.; Yakobson, B. I.; Ding, F. Efficient Defect Healing in Catalytic Carbon Nanotube Growth. *Phys. Rev. Lett.* **2012**, *108*, 245505.
(19) Reina, A.; Jia, X.; Ho, J.; Nezich, D.; Son, H.; Bulovic, V.; Dresselhaus, M. F.; Kong, J. Large Area, Few-Layer Graphene Films on Arbitrary Substrates by Chemical Vapor Deposition. *Nano Lett.* **2009**, *9*, 30−35.
(20) Li, X.; Cai, W.; An, J.; Kim, S.; Nah, J.; Yang, D.; Piner, R.; Velamakanni, A.; Jung, I.; Tutuc, E.; Banerjee, S. K.; Colombo, L.; Ruoff, R. S. Large-Area Synthesis of High-Quality and Uniform Graphene Films on Copper Foils. *Science* **2009**, *324*, 1312−1314.
(21) Bandow, S.; Takizawa, M.; Hirahara, K.; Yudasaka, M.; Iijima, S. Raman Scattering Study of Double-walled Carbon Nanotubes Derived from the Chains of Fullerenes in Single-walled Carbon Nanotubes. *Chem. Phys. Lett.* **2001**, *337*, 48−54.
(22) Su, H. B.; Nielsen, R. J.; van Duin, A.; Goddard, W. A., III. Simulations on the Effects of Confinement and Ni-catalysis on the Formation of Tubular Fullerene Structures from Peapod Precursors. *Phys. Rev. B* **2007**, *75*, 134107.
(23) Launois, P.; Chorro, M.; Verbeck, B.; Albouy, P.-A.; Rouzière, S.; Colson, D. Transformation of C_{70} Peapods into Double-walled Carbon Nanotubes. *Carbon* **2010**, *48*, 89−98.
(24) Suarez-Martinez, I.; Higginbottom, P. J.; Marks, N. A. Molecular Dynamics Simulations of the Transformation of Carbon Peapods into Double-walled Carbon Nanotubes. *Carbon* **2010**, *48*, 3592−3598.
(25) Zhang, J. Y.; Zhou, F.; Miyata, Y.; Kitaura, R.; Su, H. B.; Shinohara, H. Chirality Selective Growth and Extraction of Single-Walled Carbon Nanotubes via Fullerene Nano-Peapods. *RSC Adv.* **2013**, *3*, 16954−16957.
(26) Nikolaev, P.; Thess, A.; Rinzler, A. G.; Colbert, D. T.; Smalley, R. E. Diameter Doubling of Single-walled Nanotubes. *Chem. Phys. Lett.* **1997**, *266*, 422−426.
(27) Terrones, M.; Terrones, H.; Banhart, F.; Charlier, J.-C.; Ajayan, P. M. Coalescence of Single-Walled Carbon Nanotubes. *Science* **2000**, *288*, 1226−1229.
(28) Yoon, M.; Han, S.; Kim, G.; Lee, S. B.; Berber, S.; Osawa, E. Zipper Mechanism of Nanotube Fusion: Theory and Experiment. *Phys. Rev. Lett.* **2004**, *92*, 075504.
(29) Bougrine, A.; Dupont-Pavlovsky, N.; Naji, A.; Ghabaja, J.; Mareche, J. F.; Billaud, D. Influence of High Temperature Treatments on Single-walled Carbon Nanotubes Structure, Morphology and Surface Properties. *Carbon* **2001**, *39*, 685−695.
(30) Méténier, K.; Bonnamy, S.; Béguin, F.; Journet, C.; Bernier, P.; Lamy de La Chapelle, M. Coalescence of Single-walled Carbon Nanotubes and Formation of Multi-walled Carbon Nanotubes under High-temperature Treatments. *Carbon* **2002**, *40*, 1765−1773.
(31) López, M. J.; Rubio, A.; Alonso, J. A.; Lefrant, S.; Méténier, K.; Bonnamy, S. Patching and Tearing Single-Wall Carbon-Nanotube Ropes into Multiwall Carbon Nanotubes. *Phys. Rev. Lett.* **2002**, *89*, 255501.
(32) Kosynkin, D. V.; Higginbotham, A. L.; Sinitskii, A.; Lomeda, J. R.; Dimiev, A.; Price, B. K.; Tour, J. M. Longitudinal Unzipping of Carbon Nanotubes to Form Graphene Nanoribbons. *Nature* **2009**, *458*, 872−876.
(33) Bai, J. W.; Duan, X. F.; Huang, Y. Rational Fabrication of Graphene Nanoribbons Using a Nanowire Etch Mask. *Nano Lett.* **2009**, *9*, 2083−2087.
(34) Chu, P. K.; Li, L. Characterization of Amorphous and Nanocrystalline Carbon Films. *Mater. Chem. Phys.* **2006**, *96*, 253−277.
(35) Westenfelder, B.; Meyer, J. C.; Buskupek, J.; Kurasch, S.; Scholz, F.; Krill, C. E., III; Kaiser, U. Transformations of Carbon Adsorbates on Graphene Substrates under Extreme Heat. *Nano Lett.* **2011**, *11*, 5123−5127.
(36) Huang, J. Y. In Situ Observation of Quasimelting of Diamond and Reversible Graphite−Diamond Phase Transformations. *Nano Lett.* **2007**, *7*, 2335−2338.
(37) Asaka, K.; Karita, M.; Saito, Y. Graphitization of Amorphous Carbon on a Multiwall Carbon Nanotube Surface by Catalyst-free Heating. *Appl. Phys. Lett.* **2011**, *99*, 091907.
(38) Chen, S.; Huang, J. Y.; Wang, Z.; Kempa, K.; Chen, G.; Ren, Z. F. High-bias-induced Structure and The Corresponding Electronic Property Changes in Carbon Nanotubes. *Appl. Phys. Lett.* **2005**, *87*, 263107.
(39) Huang, J. Y.; Chen, S.; Ren, Z. F.; Chen, G.; Dresselhaus, M. S. Real-Time Observation of Tubule Formation from Amorphous Carbon Nanowires under High-Bias Joule Heating. *Nano Lett.* **2006**, *6*, 1699−1705.
(40) Barreiro, A.; Börrnert, F.; Avdoshenko, S. M.; Rellinghaus, B.; Cuniberti, G.; Rümmeli, M. H.; Vandersypen, L. M. K. Understanding the Catalyst-free Transformation of Amorphous Carbon into Graphene by Current-induced Annealing. *Sci. Rep.* **2012**, *3*, 1115.
(41) Harris, P. J. F. Solid State Growth Mechanisms for Carbon Nanotubes. *Carbon* **2007**, *45*, 229−239.
(42) Du, G.; Song, C.; Zhao, J.; Feng, S.; Zhu, Z. Solid-phase Transformation of Glass-like Carbon Nanoparticles into Nanotubes and the Related Mechanism. *Carbon* **2008**, *46*, 92−98.
(43) Zhou, D.; Chow, L. Complex Structure of Carbon Nanotubes and Their Implications for Formation Mechanism. *J. Appl. Phys.* **2003**, *93*, 9972−9976.
(44) Shakerzadeh, M.; Teo, E. N. T.; Sorkin, A.; Bosman, M.; Tay, B. K.; Su, H. Plasma Density Induced Formation of Nanocrystals in

Physical Vapor Deposited Carbon Films. *Carbon* **2011**, *49*, 1733−1744.
(45) Winter, N. W.; Ree, F. H. Carbon Particle Phase Stability as a Function of Size. *J. Comput.-Aided Mater. Des.* **1998**, *5*, 279−294.
(46) Fugaciu, F.; Hermann, H.; Seifert, G. Concentric-shell Fullerenes and Diamond Particles: A Molecular-dynamics Study. *Phys. Rev. B* **1999**, *60*, 10711−10714.
(47) Erkoç, S. From Carbon Nanotubes to Carbon Nanorods. *Int. J. Mod. Phys. C* **2000**, *11*, 1247−1255. Erkoç, S.; Malcioğlu, O. S. Structural Properties of Carbon Nanorods: Molecular Dynamics Simulations. *Int. J. Mod. Phys. C* **2002**, *13*, 367−373.
(48) Lee, G.-D.; Wang, C. Z.; Yu, J.; Yoon, E.; Ho, K. M. Heat-Induced Transformation of Nanodiamond into a Tube-Shaped Fullerene: A Molecular Dynamics Simulation. *Phys. Rev. Lett.* **2003**, *91*, 265701.
(49) Ivanovskaya, V. V.; Ivanovskii, A. L. Atomic Structure, Electronic Properties, and Thermal Stability of Diamond-like Nanowires and Nanotubes. *Inorg. Mater.* **2007**, *43*, 349−357.
(50) Powles, R. C.; Marks, N. A.; Lau, D. W. M. Self-assembly of sp^2-bonded Carbon Nanostructures from Amorphous Precursors. *Phys. Rev. B* **2009**, *79*, 075430.
(51) Okada, S.; Takagi, Y.; Kawai, T. Formation of Graphene Nanostructures on Diamond Nanowire Surfaces. *Jpn. J. Appl. Phys.* **2010**, *49*, 02BB02.
(52) Sorkin, A.; Su, H.-B.; Kang, T. B. Three-Stage Transformation Pathway from Nanodiamonds to Fullerenes. *J. Phys. Chem. A* **2011**, *115*, 8327−8334.
(53) Suarez-Martinez, I.; Marks, N. A. Amorphous Carbon Nanorods as a Precursor for Carbon Nanotubes. *Carbon* **2012**, *50*, 5441−5449.
(54) Sorkin, A.; Su, H. B. The Mechanism of Transforming Diamond Nanowires to Carbon Nanostructures. *Nanotechnology* **2014**, *25*, 035601.
(55) Marks, N. A. Generalizing the Environment-dependent Interaction Potential for Caron. *Phys. Rev. B* **2000**, *63*, 035401.
(56) Frauenheim, Th.; Weich, F.; Köhler, Th.; Uhlmann, S.; Porezag, D.; Seifert, G. Density-Functional-based Construction of Transferable Nonorthogonal Tight-binding Potential for Si and SiH. *Phys. Rev. B* **1995**, *52*, 11492−11501.
(57) Bacon, R. Growth, Structure, and Properties of Graphite Whiskers. *J. Appl. Phys.* **1960**, *31*, 283−290.
(58) Mordkovich, V. Z.; Baxendale, M.; Yoshimura, S.; Chang, R. P. H. Intercalation into Carbon Nanotubes. *Carbon* **1996**, *34*, 1301−1303.
(59) Lavin, J. G.; Subramoney, S.; Ruoff, R. S.; Berber, S.; Tománek, D. Scrolls and Nested Tubes in Multiwall Carbon Nanotubes. *Carbon* **2002**, *40*, 1123−1130.
(60) Viculis, L. M.; Mack, J. J.; Kaner, R. B. A Chemical Route to Carbon Nanoscrolls. *Science* **2003**, *299*, 1361.
(61) Braga, S. F.; Coluci, V. R.; Legoas, S. B.; Giro, R.; Galváo, D. S.; Baughman, R. H. Structure and Dynamics of Carbon Nanoscrolls. *Nano Lett.* **2004**, *4*, 881−884.
(62) Xie, X.; Ju, L.; Feng, X.; Sun, Y.; Zhou, R.; Liu, K.; Fan, S.; Li, Q.; Jiang, K. Controlled Fabrication of High-Quality Carbon Nanoscrolls from Monolayer Graphene. *Nano Lett.* **2009**, *9*, 2565−2570.
(63) Horsfield, A. P. Efficient ab initio Tight Binding. *Phys. Rev. B* **1997**, *56*, 6594−6602.
(64) Sorkin, A.; Adler, J.; Kalish, R. Nucleation of Diamond from Liquid Carbon under Extreme Pressures: Atomistic Simulation. *Phys. Rev. B* **2006**, *74*, 064115.
(65) Marks, N. A.; Cooper, N. C.; McKenzie, D. R.; McCulloch, D. G.; Bath, P.; Russo, S. P. Comparison of Density-functional, Tight-binding, and Empirical Methods for the Simulation of Amorphous Carbon. *Phys. Rev. B* **2002**, *65*, 075411.
(66) Humphrey, W.; Dalke, A.; Schulten, K. VMD - Visual Molecular Dynamics. *J. Mol. Graphics* **1996**, *14*, 33−38.
(67) Terrones, M. Nanotubes Unzipped. *Nature* **2009**, *458*, 845−846.
(68) Cano-Márquez, A. G.; Rodríguez-Macías, F. J.; Campos-Delgado, J.; Espinosa-González, C. G.; Tristán-López, F.; Ramírez-González, D.; Cullen, D. A.; Smith, D. J.; Terrones, M.; Vega-Cantú, Y. I. Ex-MWNTs: Graphene Sheets and Ribbons Produced by Lithium Intercalation and Exfoliation of Carbon Nanotubes. *Nano Lett.* **2009**, *9*, 1527−1533.
(69) Jiao, L.; Zhang, L.; Wang, X.; Diankov, G.; Dai, H. Narrow Graphene Nanoribbons from Carbon. Nanotubes. *Nature* **2009**, *458*, 877−880.
(70) Santos, H.; Chico, L.; Brey, L. Carbon Nanoelectronics: Unzipping Tubes into Graphene Ribbons. *Phys. Rev. Lett.* **2009**, *103*, 086801.
(71) Zhang, J.; Zhu, Z.; Feng, Y.; Ishikawa, H.; Miyata, Y.; Kitaura, R.; Dahl, J. E. P.; Carlson, R. M. K.; Fokina, N. A.; Schreiner, P. R.; Tománek, D.; Shinohara, H. Evidence of Diamond Nanowires Formed inside Carbon Nanotubes from Diamantane Dicarboxylic Acid. *Angew. Chem., Int. Ed.* **2013**, *52*, 3717.